

Supplementary Results

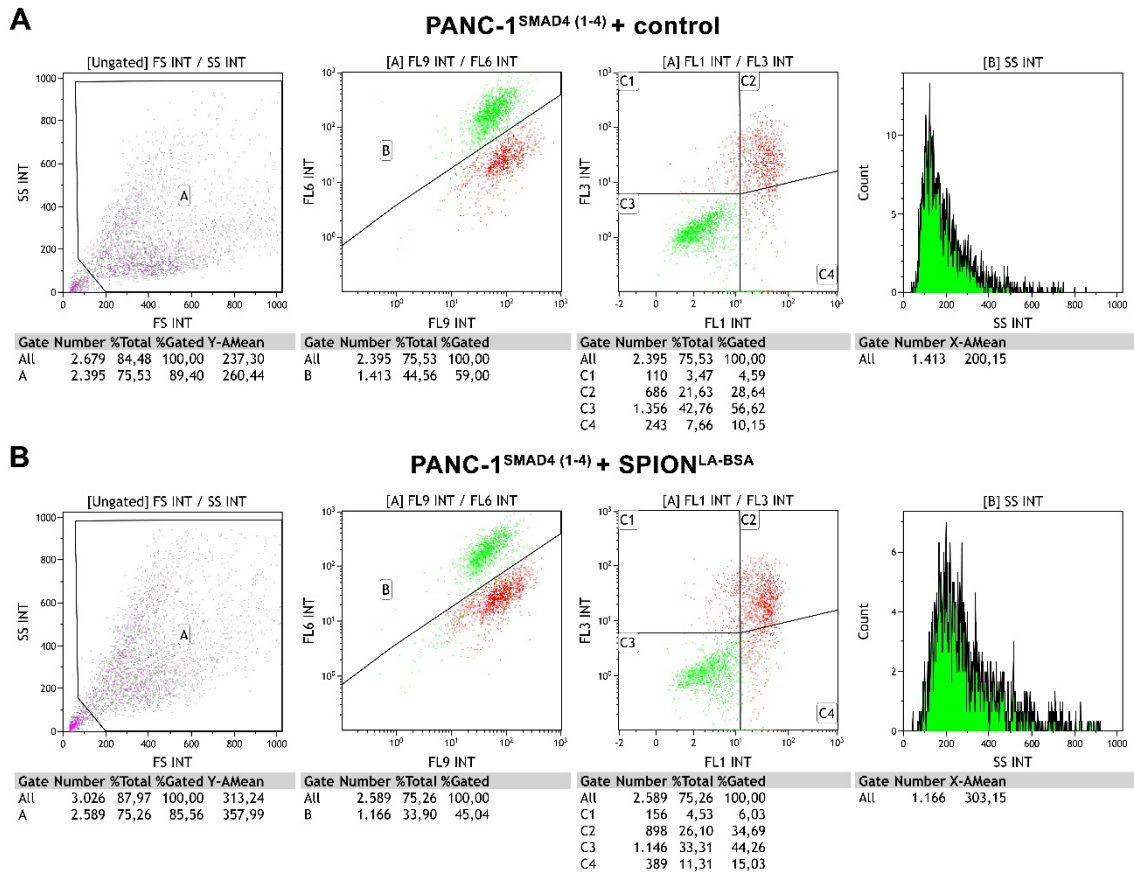
Intracellular quantification and localization of label-free iron oxide nanoparticles by holotomographic microscopy

Ralf P. Friedrich¹, Eveline Schreiber¹, Rainer Tietze¹, Hai Yang², Christian Pilarsky², Christoph Alexiou¹

¹Department of Otorhinolaryngology, Head and Neck Surgery, Section of Experimental Oncology and Nanomedicine (SEON), Else Kröner-Fresenius-Stiftung Professorship, Universitätsklinikum Erlangen, Erlangen 91054, Germany

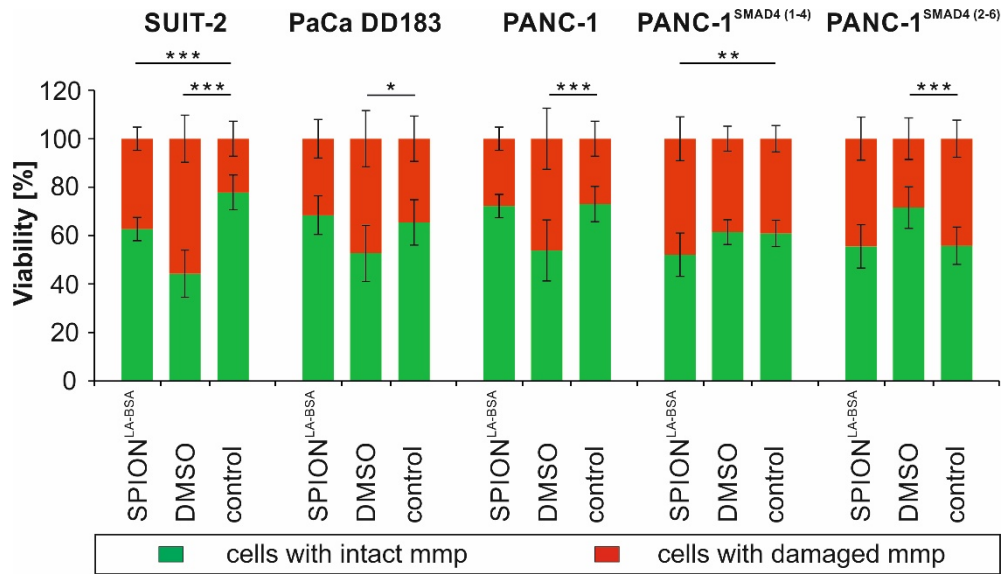
²Department of Surgery, Universitätsklinikum Erlangen, Erlangen 91054, Germany.

Correspondence: Ralf P. Friedrich
Glückstrasse 10a, 91054 Erlangen, Germany
Tel +49 9131 85 43943
Fax +49 9131 85 34828
Email ralf.friedrich@uk-erlangen.de



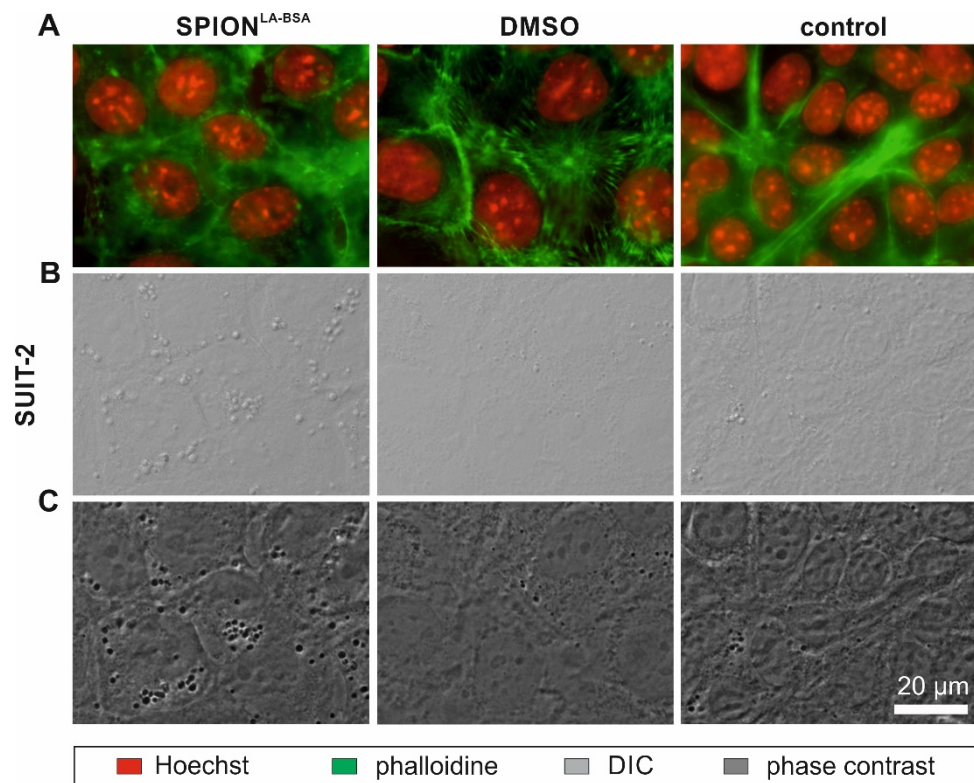
Supplementary Figure S1 Gating strategy of the flow cytometry experiments. Shown are representative plots and histograms of (A) PANC-1^{SMAD4 (1-4)} cells treated with the corresponding amount of H₂O instead of SPIONs and (B) PANC-1^{SMAD4 (1-4)} cells treated with 100 µg_{Fe}/ml SPION^{LA-BSA} for 24 h. Gate A in the first column shows all events without free particles, particle agglomerates and cell debris originating from the necessary intensive treatment for cell detachment. Second column is gated on A, where DiIC1(5) (FL6 INT) is plotted against Hoechst (FL9 INT). The upper population (gate B) represents cells with intact mitochondrial membrane potential, whereas the lower population shows cells with damaged membrane potential. The third column is gated on A, where propidium iodide (FL3 INT) is plotted against annexin V-FITC (FL1 INT). The population in gates C1 and C2 represents necrotic cells, C3 viable cells and C4 apoptotic cells. The last column shows histograms of the side scatter (SS) gated on viable cells in gate B. An increase in the arithmetic mean (X-A-Mean) of the side scatter intensity (SS INT) correlates with an increase in the cellular SPION amount.

Abbreviations: SPION, superparamagnetic iron oxide nanoparticles; SPION^{LA-BSA}, lauric acid- and bovine serum albumin-coated SPIONs.



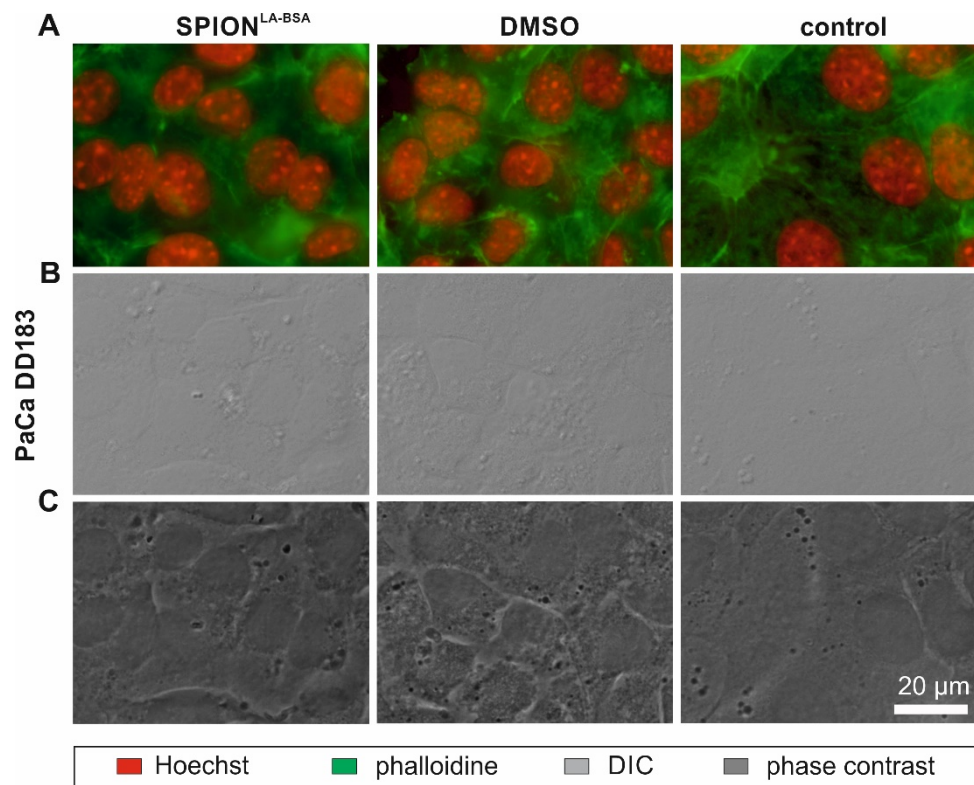
Supplementary Figure S2 Status of the mitochondrial membrane potential (mmp) after SPION treatment. Cells were incubated for 24 h with 100 μg_{Fe} /ml SPION^{LA-BSA}. Cell viability was determined by DiIC1(5) staining and analyzed by flow cytometry. The amount of cells with intact mmp viable (DiIC1(5)+), and cells containing a defect mmp (DiIC1(5)-) are shown for SUIT-2, PaCa DD183, PANC-1, PANC-1^{SMAD4 (1-4)} and PANC-1^{SMAD4 (2-6)}. Toxicity controls contain 2% DMSO, negative controls represent the corresponding amount of H₂O instead of water-based ferrofluid. Data are expressed as the mean \pm standard deviation (n=4 with technical quadruplicates). Statistical significance in the percentage of cells with intact mmp are indicated with *, ** and ***. The respective confidential intervals are $p < 0.002$, $p < 0.0002$ and $p < 0.00002$ and were calculated via t-test analysis.

Abbreviations: SPION, superparamagnetic iron oxide nanoparticles; SPION^{LA-BSA}, lauric acid- and bovine serum albumin-coated SPIONs; mmp, mitochondrial membrane potential; DMSO, Dimethyl sulfoxide.



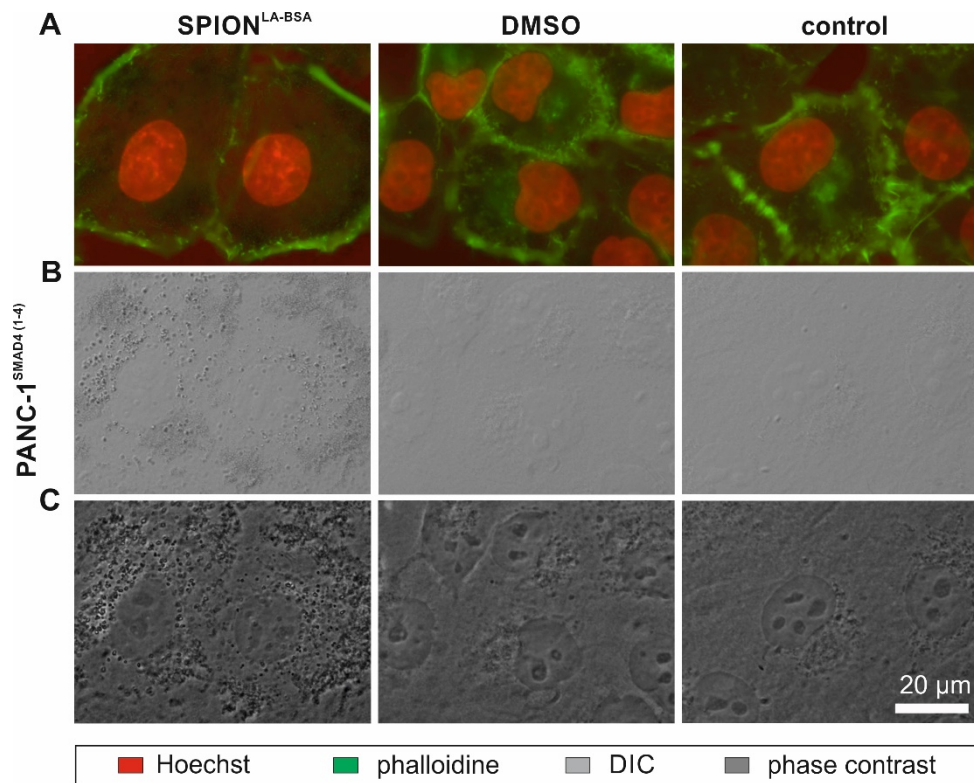
Supplementary Figure S3 SPION load visualized by optical imaging. SUIT-2 cells were treated with unlabeled SPION^{LA-BSA} (100 μg_{Fe}/ml) or with the corresponding amount of H₂O or DMSO (final concentration of 2%) for 24 h and visualized by (A) fluorescent staining for nuclei (Hoechst 33342, red) and actin cytoskeleton (Alexa Fluor 488 Phalloidin, green), (B) differential interference contrast (DIC) and (C) phase contrast. Compared to few spots with high contrast within control and DMSO samples, numerous areas of high contrast indicate SPION accumulations within vesicles in nanoparticle treated cells.

Abbreviations: SPION, superparamagnetic iron oxide nanoparticles; SPION^{LA-BSA}, lauric acid- and bovine serum albumin-coated SPIONs; DMSO, Dimethyl sulfoxide; DIC, Differential interference contrast.



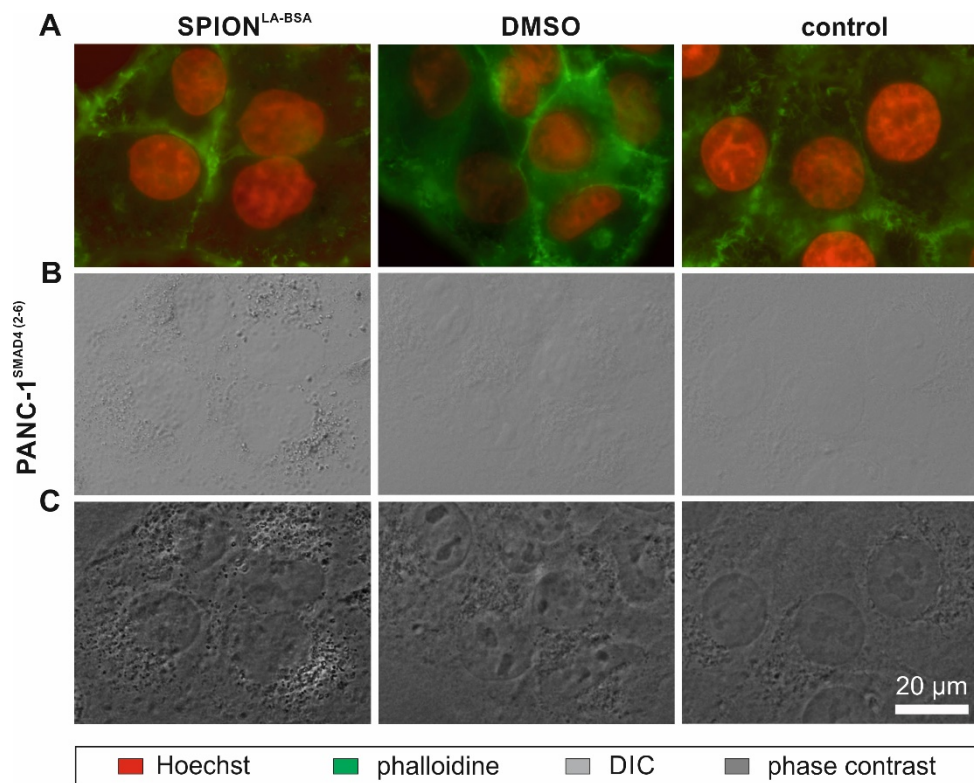
Supplementary Figure S4 SPION load visualized by optical imaging. PaCa DD183 cells were treated with unlabeled SPION^{LA-BSA} (100 $\mu\text{g}_{\text{Fe}}/\text{ml}$) or with the corresponding amount of H₂O or DMSO (final concentration of 2%) for 24 h and visualized by (A) fluorescent staining for nuclei (Hoechst 33342, red) and actin cytoskeleton (Alexa Fluor 488 Phalloidin, green), (B) differential interference contrast (DIC) and (C) phase contrast. Compared to few spots with high contrast within control and DMSO samples, numerous areas of high contrast indicate SPION accumulations within vesicles in nanoparticle treated cells.

Abbreviations: SPION, superparamagnetic iron oxide nanoparticles; SPION^{LA-BSA}, lauric acid- and bovine serum albumin-coated SPIONs; DMSO, Dimethyl sulfoxide; DIC, Differential interference contrast.



Supplementary Figure S5 SPION load visualized by optical imaging. PANC-1^{SMAD4 (1-4)} cells were treated with unlabeled SPION^{LA-BSA} (100 μg_{Fe}/ml) or with the corresponding amount of H₂O or DMSO (final concentration of 2%) for 24 h and visualized by **(A)** fluorescent staining for nuclei (Hoechst 33342, red) and actin cytoskeleton (Alexa Fluor 488 Phalloidin, green), **(B)** differential interference contrast (DIC) and **(C)** phase contrast. Compared to few spots with high contrast within control and DMSO samples, numerous areas of high contrast indicate SPION accumulations within vesicles in nanoparticle treated cells.

Abbreviations: SPION, superparamagnetic iron oxide nanoparticles; SPION^{LA-BSA}, lauric acid- and bovine serum albumin-coated SPIONs; DMSO, Dimethyl sulfoxide; DIC, Differential interference contrast.



Supplementary Figure S6 SPION load visualized by optical imaging. PANC-1^{SMAD4 (2-6)} cells were treated with unlabeled SPION^{LA-BSA} (100 μg_{Fe}/ml) or with the corresponding amount of H₂O or DMSO (final concentration of 2%) for 24 h and visualized by **(A)** fluorescent staining for nuclei (Hoechst 33342, red) and actin cytoskeleton (Alexa Fluor 488 Phalloidin, green), **(B)** differential interference contrast (DIC) and **(C)** phase contrast. Compared to few spots with high contrast within control and DMSO samples, numerous areas of high contrast indicate SPION accumulations within vesicles in nanoparticle treated cells.

Abbreviations: SPION, superparamagnetic iron oxide nanoparticles; SPION^{LA-BSA}, lauric acid- and bovine serum albumin-coated SPIONs; DMSO, Dimethyl sulfoxide; DIC, Differential interference contrast.

technique	+/- SPION	SUIT-2	PaCa DD183	PANC-1	PANC-1 ^{SMAD4 (1-4)}	PANC-1 ^{SMAD4 (2-6)}
holotomographic microscopy RI int./ μm^3	+	2.35 ± 1.43	2.95 ± 1.13	2.46 ± 1.48	6.34 ± 3.82	10.93 ± 4.60
	-	0.90 ± 0.61	2.84 ± 1.00	1.04 ± 0.35	1.91 ± 0.94	0.82 ± 0.70
MP-AES pg _{Fe} /cell	+	0.64 ± 0.13	0.59 ± 0.25	0.64 ± 0.19	17.93 ± 2.41	22.39 ± 4.04
	-	0.12 ± 0.05	0.07 ± 0.03	0.11 ± 0.03	0.21 ± 0.11	0.22 ± 0.07
flow cytometric side scatter analysis arithmetic mean	+	153.8 ± 8.2	159.9 ± 11.6	205.0 ± 41.5	242.9 ± 22.2	231.8 ± 35.8
	-	101.6 ± 6.6	123.5 ± 7.2	150.7 ± 26.2	168.4 ± 17.3	161.2 ± 19.8

Supplementary Table S1 Comparison of data achieved by holotomographic microscopy, MP-AES and flow cytometric side scatter analysis. Different cell lines were treated with 100 $\mu\text{g}_{\text{Fe}}/\text{ml}$ SPION^{LA-BSA} (+) or with the corresponding amount of H₂O (-) for 24 h. Cellular SPION amount were represented as the increase of RI int./ μm^3 , pg_{Fe}/cell and side scatter, quantified using holotomography, MP-AES and flow cytometry, respectively. Compared to the control, SPION-treatment resulted in a very strong increase of the different data sets in PANC-1^{SMAD4 (1-4)} and PANC-1^{SMAD4 (2-6)}, whereas the increase with other cell lines were significantly slighter and not that pronounced. Together, the data show a clear correlation of the measured SPION amounts between all methods.

Abbreviations: SPION, superparamagnetic iron oxide nanoparticles; SPION^{LA-BSA}, lauric acid- and bovine serum albumin-coated SPIONs; MP-AES, microwave plasma-atomic emission spectroscopy; RI int., intensity of the refractive index above a defined threshold.